Separation and Purification Technology 353 (2025) 128376

Contents lists available at ScienceDirect

Separation and Purification Technology

journal homepage: www.elsevier.com/locate/seppur

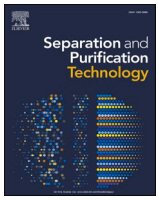

Mechanistic study of cefixime degradation with an atmospheric air dielectric barrier discharge – Influence of radical scavengers and metal ion catalyst

Samuel O. Babalola [a], Paul A. Steenkamp [b], Michael O. Daramola [a], Samuel A. Iwarere [a,*]

[a] University of Pretoria, Department of Chemical Engineering, Faculty of Engineering, Built Environment and Information Technology, Hatfield, Pretoria 0002, South Africa
[b] Centre for Plant Metabolomics Research, Department of Biochemistry, University of Johannesburg, Auckland Park, Johannesburg 2006, South Africa

ARTICLE INFO

Editor: G. Chen

Keywords:
Cefixime
Radical scavengers
Degradation efficiency
Metal ion catalyst
DBD plasma

ABSTRACT

The ineffective removal of antibiotic residues and their metabolites by conventional wastewater treatment setups lead to their continuous discharge into the environment, causing risks to both aquatic life and human health. This study explored the use of a non-thermal plasma (NTP) generated by atmospheric air for the degradation of cefixime (CFX), a widely consumed and recalcitrant antibiotic. This study achieved a complete degradation of CFX using an NTP technology in 8 min treatment time at 6 kV and 20 kHz applied AC voltage and frequency, respectively using a high voltage alternating current power supply unit. An energy yield of 0.42 g/kWh was estimated. The degradation of the pollutant was influenced by solution flow rate, applied voltage and the solution characteristics. Five degradation by-products were identified based on quadrupole time-of-flight (Q-TOF) mass spectrum (MS) analysis and a possible degradation pathway for the pollutant was proposed. Also, radical scavenger experiments were set up to understand the specific chemical species facilitating CFX degradation. The effect of Fe^{2+} catalyst on the degradation of CFX was investigated in the aqueous solution. This low-cost metal ion catalyst has been known to improve the degradation of organic compounds by facilitating the oxidizing power of H_2O_2. Considering this, a new idea was examined in this study which was the degradation of the antibiotic in the presence of both Fe^{2+} catalyst and some radical scavengers (*iso*-propyl alcohol – IPA, *tert*-butyl alcohol – TBA, and sodium hydrogen carbonate – $NaHCO_3$). When Fe^{2+} was introduced into CFX solutions containing TBA, IPA and $NaHCO_3$, respectively, the degradation and kinetics increased by at least 33 %. In these mixed additives, the degradation of the pollutant was enhanced by the consumption of H_2O_2.

1. Introduction

Cefixime (CFX), an antibiotic belonging to the cephalosporin class, has been included in some lists of emerging contaminants that are being monitored by regulatory agencies in water and wastewater [1]. It is widely prescribed for the treatment of bacterial infections in humans, including respiratory tract infections, urinary tract infections, and sexually transmitted infections. Due to its frequent use and incomplete absorption in the body, a significant amount of CFX is excreted through urine and this ends up in wastewater [2]. Meanwhile, conventional wastewater treatment processes have not been effective in removing most antibiotics. As a result, significant quantities of CFX pass through these treatment systems and enter the environment through effluent discharge. In the environment, CFX exhibits moderate to high persistence, leading to their long-term presence. At the same time, prolonged exposure to CFX and other similar persistent antibiotics has been linked to developmental abnormalities, reduced reproductive success, disruptions in the balance of microbial ecosystems in aquatic environments, and the development of antibiotic resistance [3].

As emerging technologies like advanced oxidation processes (AOPs) continue to gain interest in the degradation of refractory organic pollutants, plasma generated in electrical discharges has also been investigated as a possible degradation method for antibiotics since it leaves less toxic by-products. Plasma formation occurs through the introduction of energy into the gaseous phase, initiating inelastic collisions that lead to ionization and dissociation processes [4]. The most captivating

* Corresponding author.
E-mail address: samuel.iwarere@up.ac.za (S.A. Iwarere).

https://doi.org/10.1016/j.seppur.2024.128376
Received 28 November 2023; Received in revised form 8 June 2024; Accepted 9 June 2024
Available online 13 June 2024

aspect of plasma lies in its capacity to establish a dynamic environment where photons, electrons, positive ions, reactive species (excited molecules and atoms), and radicals can coexist simultaneously [5]. As a collective entity, plasma demonstrates macroscopic neutrality and exhibits synergistic behaviour. Non-thermal plasma (NTP) reactor designs like corona discharges [6–9], dielectric barrier discharge (DBD) [10–12], gliding arc [13,14], glow discharges [15], have already been used in the degradation of recalcitrant microorganic compounds in water. In each geometry, the plasma is generated either within the liquid or in the gas phase above the liquid, or in some cases, in both the liquid and gas phases. Discharges generated in the liquid or gas phase result in different physical and chemical effects, which include the formation of shock waves, UV radiation, active radicals (•H, •O, •OH), and molecular species (H_2O_2, O_3, etc.) [16]. A DBD plasma technology provides a novel means by which all these species can be generated at relatively low temperatures and with high energy efficiency. Non-biodegradable pharmaceutical pollutants like pentoxifylline [16], ibuprofen [17], ciprofloxacin [18], norfloxacin [19], diclofenac [20], carbamazepine, [21] amongst others have been significantly degraded using a DBD reactor.

While DBD plasma is known for its energy efficiency, it is worth noting that the plasma characteristics can be significantly influenced by certain operating conditions. For instance, to improve the efficiency of a DBD plasma-based water treatment process, researchers have combined DBD plasma with other technologies like an ultrafiltration system for low energy degradation [22] or increased the mass transfer of the reactive species from the gas to the liquid phase through underwater bubbles [23]. The use of innovative power sources has also improved energy efficiency [24,25]. To increase the chances of deploying the DBD system beyond lab-scale scale applications, some studies have examined the effect of water recirculation for increased throughput [8]. The use of heterogeneous catalysts like TiO_2 and CeO_2 has also been widely used to increase the generation of reactive species by leveraging on their activation with UV radiation and conversion of long-lived species into highly reactive ones (•OH) [26–29]. However, these catalysts impose a high cost of treatment and the need to add a catalyst-recovery step all of which make their industrial applications a challenge to date. On the other hand, some studies have noted that the inclusion of a metal ion catalyst could potentially improve degradation efficiency with lower associated costs [30–32].

In attempting to understand the controlling effect of active radicals, the degradation of pollutants in the presence of radical scavengers has also been explored, and the results have shown that radical scavengers could impede or enhance the degradation of a pollutant, depending on the active residual chemical species [10,33,34]. Also, the feed gas composition shows a remarkable effect on the treatment process during plasma treatment. For instance, Zhang et al. [35] compared the degradation efficiency of antibiotic CFX with oxygen, synthetic air, nitrogen, and argon using an underwater bubble DBD technology operated in batch mode. The authors reported that in the presence of synthetic air, the removal of CFX reached as high as 94.8 %, next to oxygen (99.8 %), in 30 min treatment time. Argon and Nitrogen gases gave a degradation efficiency of 73.4 % and 45.3 %, respectively. Besides this being the only available literature on CFX degradation with NTP, the degradation experiments in this study were conducted in a batch reactor and in a small volume. To the best of our knowledge, there is no study on the removal of CFX with a continuous-flow DBD plasma generated by natural atmospheric air. The intrinsic advantage of running a plasma experiment with natural air lies in the reduction of its cost of treatment which boosts its potential for commercial deployment. Also, there is an underexplored area in plasma water treatment and AOPs in general which is the investigation of the technology's performance in the presence of low-cost metal ion catalysts and radical scavengers.

Therefore, the contribution of this study is threefold. First, a continuous-flow atmospheric air DBD plasma was used to study the degradation of CFX for the first time. Secondly, after optimizing the factors that affect the degradation of the pollutant, an investigation of the reactive species facilitating this process was conducted. The intermediate products identified during the degradation process with the key reactive species provided a hint on the possible removal mechanism for CFX. Lastly, the influence of a catalytic metal ion (Fe^{2+}) was studied as well as its effect in enhancing the degradation of CFX in the presence of various OH radical scavengers. Considering the interrelationship between •OH and H_2O_2, the concentration of H_2O_2 was monitored in the synthetic solutions containing •OH scavengers and the metal ion catalyst. Overall, the main results from this study suggest a method for significantly increasing the efficiency of a DBD plasma technology in handling persistent micropollutants like antibiotic cefixime whilst also potentially reducing the cost of treatment.

2. Experimental section

2.1. Materials and chemicals

Cefixime ($C_{16}H_{15}N_5O_7S_2$ and MW = 453.45 g/mol) was purchased from Sigma-Aldrich Company (Germany). The physicochemical properties and chemical structure of CFX are summarized in Table S1 and Fig. S1, respectively. Iron (II) sulphate heptahydrate ($FeSO_4{\cdot}7H_2O$) used as the source of Fe^{2+} was purchased from Merck, Germany. The chemical reagents used as radical scavengers include *iso*-propyl alcohol ($(CH_3)_2CHOH$) supplied by Radchem (PTY) LTD (South Africa), *tert*-butyl alcohol ($(CH_3)_2CHOH$), sodium hydrogen carbonate ($NaHCO_3$), sodium pyruvate ($C_3H_3NaO_3$), p-benzoquinone ($C_6H_4O_2$) and uric acid ($C_5H_4N_4O_3$) which were supplied by Sigma-Aldrich (USA). The pH of the solution was altered using sodium hydroxide (NaOH) and sulphuric acid (H_2SO_4) which were purchased from Glassworld (South Africa). All the chemicals used were of high-purity analytical grade and therefore required no further purification. The working solutions were prepared in deionized water obtained using an Elga LabWater PURELAB® Chorus 1 device.

2.2. Experimental procedure

The experimental set-up for this study is provided in Fig. 1. The major instruments consist of a DBD plasma reactor with water-falling film, high voltage AC power supply, high-performance liquid chromatography (HPLC), an ultra-performance liquid chromatography (UPLC) −quadrupole time–of–flight (Q-TOF) mass spectrometer (MS), and a digital oscilloscope. To characterize the plasma generated, both the digital oscilloscope and an optical emission spectrometer (OES) were used. Some of the species generated by the DBD plasma reactor with atmospheric air include N_2, •OH, N_2^+, and O as shown in their excited forms in Fig. S2. These were also extensively discussed in our previous study [36]. The DBD reactor itself as shown in Fig. S3 consists of a high voltage electrode made of a multi-pin stainless steel rod of 29 cm in length and 1.27 cm in diameter. This was placed in a 30 cm long borosilicate glass tube which has 0.23 cm wall thickness and 4 cm outer diameter. The outer electrode was made of conductive copper tape with a 1 mm width and a thickness of 0.1 mm. The DBD plasma discharge was generated with natural atmospheric air in the absence of any aerodynamic device with a 6.9 mm discharge length. The CFX solution was circulated in and out of the reactor by a peristaltic pump operated at a 500 mL/min flow rate. The synthetic CFX solution enters the reactor through the hollow HV electrode and is sprayed via a micro jet spray centrally positioned at the top of the reactor. As the solution falls within the reactor, it contacts the plasma discharge generated at the multi-pins where the reactive species are able to act on the contaminant.

100 mg/L stock solution of CFX was prepared in 1 L deionized water and subjected to sonication for about 20 min. Subsequently, 5 mg/L of CFX in 500 mL working solutions were derived from the stock solution. The experiments were conducted in continuous flow mode and at predetermined time intervals, samples of the treated solution were

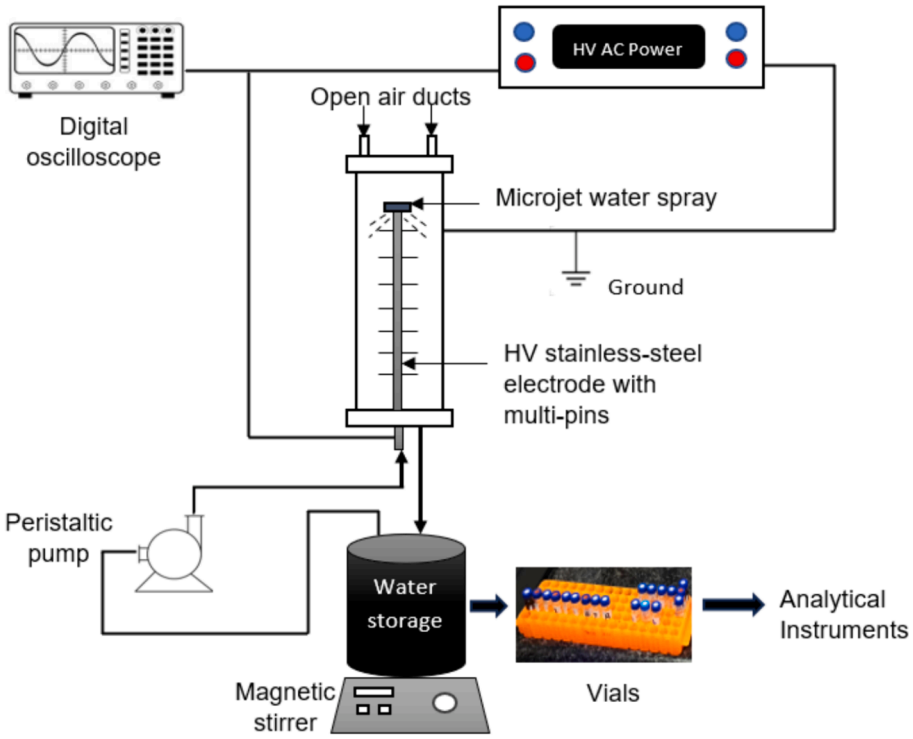

Fig. 1. Experimental setup for the DBD plasma system.

withdrawn from the water storage for both quantitative and qualitative analysis. The AC input voltage considered are 4, 5, and 6 kV and at a frequency of 20 kHz. Each experiment was conducted either in duplicate or triplicate, and the reported values represent the mean along with their error bars.

2.3. Analytic methods

A Waters Alliance (2695 series) HPLC system equipped with Waters C18 5μ column (4.6 mm × 250 mm) was used to analyze the concentration of CFX during the experiments. The mobile phase consisted of 25 % acetonitrile and 75 % water (with 1 % acetic acid) and a flow rate of 1 mL/min was used. The injection volume was 10 μL while the column temperature was set at 30 ± 5 ℃. A Waters UV–Vis detector was used, and this was set at 289 nm. The degradation efficiency was calculated as:

$$\eta = \frac{C_o - C_t}{C_o} \times 100 \quad (1)$$

where η is the degradation efficiency of CFX, C_o is the initial concentration of CFX (mg/L) and C_t is the concentration of CFX (mg/L) at treatment time t (min). The kinetic analysis of CFX with DBD plasma was fitted according to the following first-order kinetic Eq. (2).

$$In\left(\frac{C_o}{C_t}\right) = kt \quad (2)$$

Where k is the reaction rate constant (min^{-1}), t is the treatment time (min). The efficiency of the pollutant degradation was represented by the energy yield (Y, g/kWh) which is defined as the amount of CFX degraded per unit energy consumed in the discharge according to Eq. (3) [16,37].

$$(Y^*, g/kWh) = \frac{C_o V \eta}{Pt} \quad (3)$$

Where V is the volume of the solution treated (mL); P is the average power dissipated in the discharge (W). The average power dissipated was calculated using Eq. (4).

$$P(W) = \frac{I}{T}\int_0^T V(t) \times I(t)\,dt \quad (4)$$

Where V(t) and I(t) represent the voltage and current measured by the digital oscilloscope per time, respectively, while the period is represented as T (min). A representation of the current and voltage waveforms at 6 kV and 20 Hz frequency is shown in Fig. S4. The power computed in this study ranges from 27 – 42.7 W, depending on the applied voltage.

The pH measurements were taken with a HANA multiparameter H198194 meter. The concentrations of H_2O_2 and O_3 generated in the plasma discharge were measured with a Lovibond spectrodirect water testing instrument (Tintometer Group, Germany), while an ion chromatography (IC) with a metrosep C6-250/4 separation column and C6 eluent 8 mM oxalic acid was used to determine the concentrations of both NO_2^- and NO_3^- in the aqueous solution during DBD treatment. To investigate the roles of the active species generated in the plasma, scavenger experiments were set up with individual solutions of CFX containing uric acid (UA), *tert*-butyl alcohol (TBA), p-benzoquinone (BQ), and sodium pyruvate (SP) to trap O_3, •OH, $•O_2^-$ and H_2O_2, respectively.

2.4. Byproduct identification

A Waters UPLC coupled in series to a Waters SYNAPT G1 HDMS mass spectrometer was used to generate accurate mass data for the degradation byproducts. Optimization of the chromatographic separation was done utilizing a Waters HSS T3 C18 column (150 mm x 2.1 mm, 1.8 μm), and the column temperature was controlled at 60 °C. A binary solvent mixture was used consisting of water (Eluent A) containing 10 mM formic acid (pH of 2.4) and acetonitrile (Eluent B) containing 10 mM formic acid. The initial conditions were 98 %A at a flow rate of 0.4 mL/min and were maintained for 1 min, followed by a linear gradient to 10 %A at 6 min. The conditions were kept constant for 1 min and then changed to the initial conditions. The runtime was 10 min, and the injection volume was 1 μL. Samples were kept cool at 8 °C in the Waters

Sample Manager during the analysis.

For the TOF mass spectrometry analysis, a SYNAPT G1 mass spectrometer was used in V-optics and operated in electrospray mode to enable the detection of all ESI-compatible compounds. Leucine enkephalin (50 pg/mL) was used as a reference calibrant (Lock Mass) to obtain typical mass accuracies between 1 and 5 mDalton (mDa). The mass spectrometer was operated in both ESI positive and negative modes with a capillary voltage of 2.5 kV, the sampling cone at 30 V, and the extraction cone at 4.0 V. The scan time was 0.2 sec covering the 50 to 1000 Dalton mass range with an interscan time of 0.02 sec. The source temperature was 120 °C and the desolvation temperature was set at 450 °C. Nitrogen gas was used as the nebulization gas at a flow rate of 550 L/h and cone gas was added at 50 L/h. The software used to control the hyphenated system and do all data manipulation was MassLynx 4.1 (SCN 872).

3. Results and discussion

3.1. Impact of solution water flow rate

In a continuous-flow scenario, the flow rate of the treated solution influences the circulation time of the solution as well as the thickness of the liquid film. Therefore, in this study, the impact of solution flow rate on the removal of CFX was investigated as shown in Fig. 2 (a) and (b). An increase in the flow rate from 300 mL/min to 500 mL/min favoured the removal of CFX from 94 % to over 99 %, and the *k* increased from 0.32 min^{-1} to 0.58 min^{-1}, respectively. This is because an increase in the rate of recirculation of the treated solution in the reactor increased the thickness of the liquid film thus reducing the loss of reactive species. Also, increasing the flow rate of the liquid increased the number of possible cycle times of the solution within the reactor thus enhancing the degradation of the targeted pollutant by adequate contact with the reactive species. This observation was also reported in the removal of Ibuprofen [38] and N, N-diethyl-m-toluamide (DEET) [39] by a water-falling film DBD plasma. In practical applications, a high flow rate will be necessary for treating a high volume of solution. However, at a very high flow rate, the liquid film might become too thick for the formation of the discharge and distribution of the reactive species. This can reduce the degradation efficiency and kinetics as was observed in Fig. 2 (a) and (b) with a 600 mL/min flow rate. Considering the degradation efficiency and rate constant shown by the *k* value, the water flow rate for later experiments was set at 500 mL/min.

3.2. Impact of applied voltage

The influence of applied voltage is an important factor in plasma treatment, particularly due to its influence on the concentration of reactive species that oxidize pollutants in the aqueous solution. Generally, an increase in the applied voltage leads to the production of more reactive species which will enhance the rate of pollutant removal. The effect of applied voltage on CFX removal is shown in Fig. 3 under the influence of the optimized flow rate (500 mL/min) and initial CFX concentration of 5 mg/L. With an increase in the input voltage from 4 kV to 6 kV, the degradation efficiency for the pollutant rose from 40 % to over 99 % within the 8 min of treatment, respectively as shown in Fig. 3 (a). Concurrently, as shown in Fig. 3 (b), the kinetic constant increased by an order of magnitude (from 0.05 min^{-1} to 0.58 min^{-1}) as the applied voltage increased from 4 kV to 6 kV. An increase in the intensity of the reactive species was confirmed by an elongation of the spark purple discharges into long streamers as the voltage increased from 4 kV to 6 kV. The long streamers generated at 6 kV led to a faster degradation of CFX. During the treatment, the temperature of the electrode and that of the solution remained at about 25 ± 0.6 ℃, indicating that the degradation occurred at a low temperature.

The relationship between energy yield and the treatment time is shown in Fig. S5 (a). Across specific voltages, the energy yield decreased as the treatment progressed. After 8 min plasma treatment, the energy yields recorded for 4 kV, 5 kV, and 6 kV were 0.19 g/kWh, 0.34 g/kWh, and 0.42 g/kWh, respectively. The degradation efficiency and energy yields for different AOPs used in the removal of CFX were compared in Table 1. The DBD plasma used in this study had the shortest treatment time taken to attain over 90 % degradation efficiency among the technologies. Also, the energy yield recorded in this study far surpassed what was reported in most of the studies presented. Zhang et al. [35] reported a 1.5 g/kWh energy yield for CFX degradation using an underwater plasma bubble reactor in 50 mL solution after 30 min.

3.3. Impact of CFX concentration

Typically, the concentration of organic pollutants in the environment varies over time due to various reasons, as discussed in Verlicchi et al. [40]. Therefore, it is necessary to examine the effect of different CFX concentrations on its degradation. The concentration of CFX is related to the number of molecules of the compound in the solution which in turn affects its reaction with the active species generated by the DBD plasma reactor. The effect of the initial concentration of CFX was investigated at an optimum flow rate of 500 mL/min and applied voltage of 6 kV. From Fig. 4, a lower initial concentration of CFX aided the degradation of the

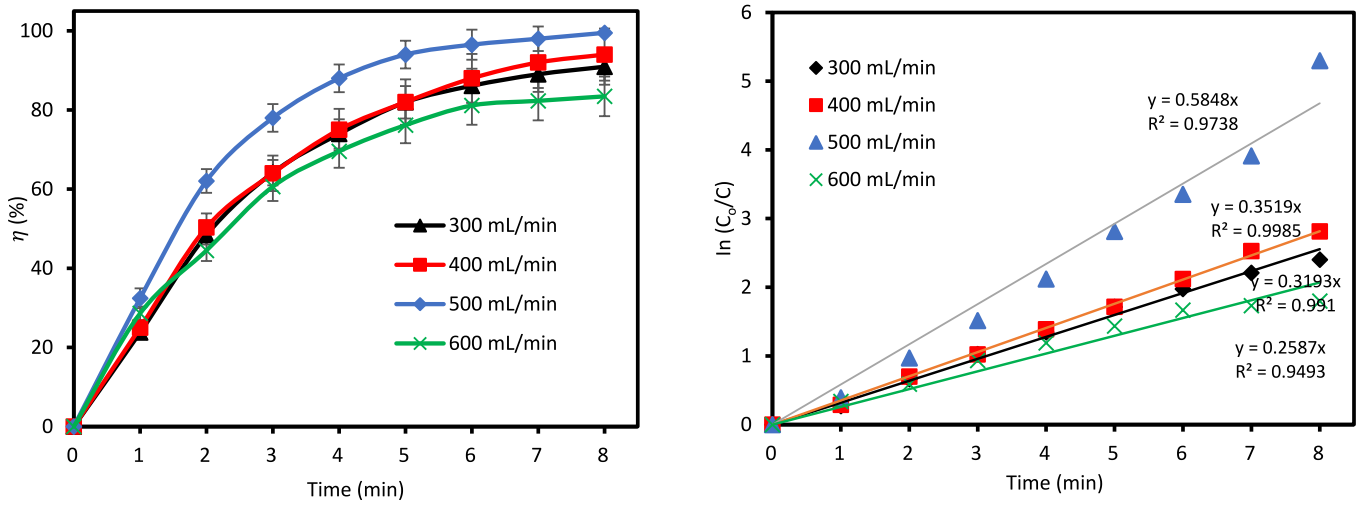

Fig. 2. Effect of water flow rate (a) degradation efficiency (b) kinetics (Input voltage: 6 kV, initial concentration of CFX: 5 mg/L).

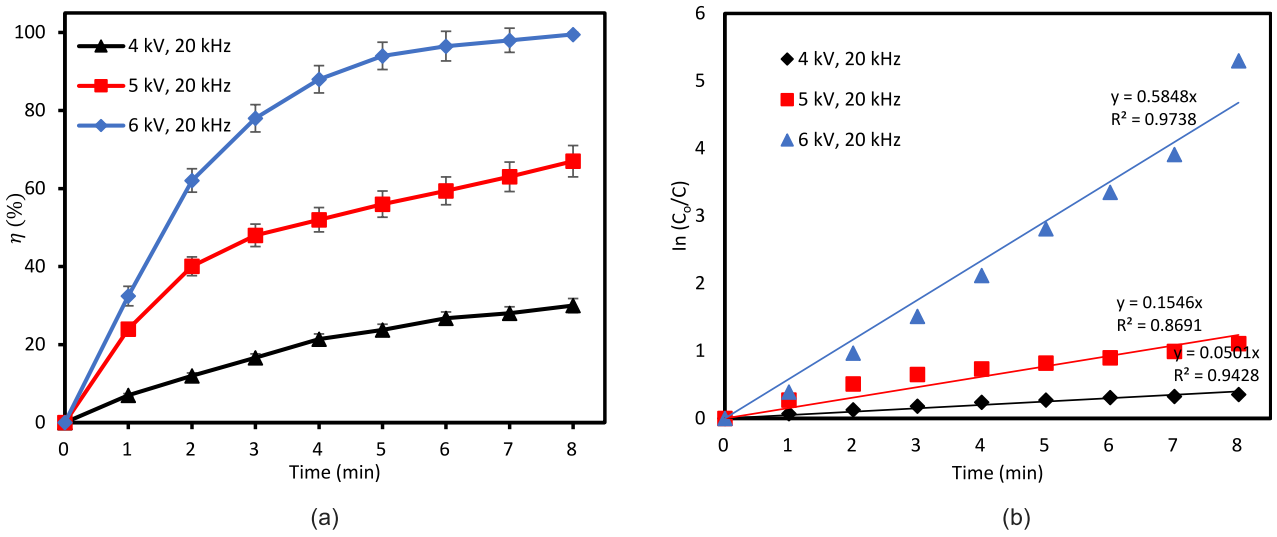

Fig. 3. Effect of applied voltage (a) degradation efficiency (b) kinetics (flow rate: 500 mL/min, initial concentration of CFX: 5 mg/L).

Table 1
Comparison between selected AOPs used in the degradation of cefixime.

Technology	Operating conditions	Initial concentration (mg/L)	Treatment time (min)	Degradation efficiency (%)	Energy yield (g/kWh)	Reference
SWCNT/ZnO/Fe_3O_4 catalyst under UV-A irradiation	0.46 g/L of the photocatalyst at pH 5.93	10	180	94.19	–	[42]
Photo-Fenton system	$NiCu_2S_4$ QDs@Fe_3O_4 nanocomposite using visible light	20	180	81	–	[43]
CuO-NiO nanocomposite	1 g/L of the photocatalyst at pH 2	15.22	180	90	–	[44]
Nano α-Fe_2O_3/ZnO photodegradation	0.41 g/L of the catalyst under 8 W/m^2 UV–vis irradiation	10.11	127	99.1	0.022	[45]
NiO/nano-clinoptilolite (NiO/NCP)	0.25 g/L of the photocatalyst at pH 5	20	300	80	0.043	[46]
Visible-light photocatalysis using α-Fe2O3@TiO2	0.012 g/L of the catalyst at pH 4.76 and calcination temperature of 439.34 °C	20.5	103	98.8	–	[47]
Plasma bubbles generated under water	Batch operation with discharge power of 6.3 W	100	30	94.8	1.5	[35]
DBD plasma discharge with multi-pin electrode	Atmospheric DBD plasma operated in continuous flow mode	5	8	>99	0.42	This work

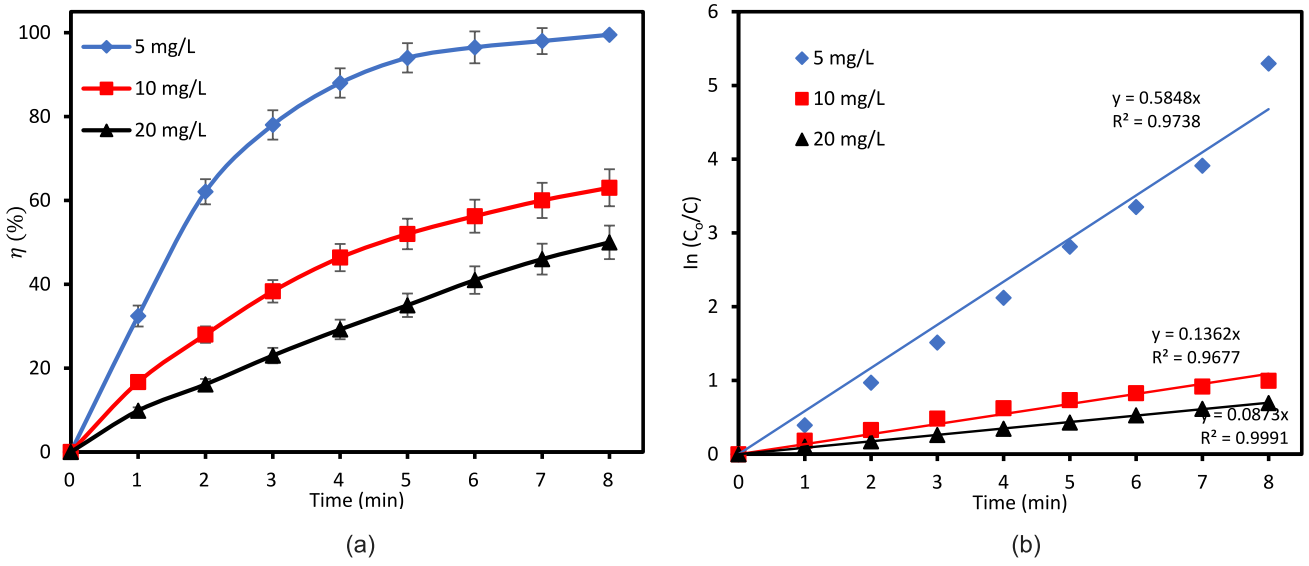

Fig. 4. Effect of input concentration (a) degradation efficiency (b) kinetics (flow rate: 500 mL/min, input voltage: 6 kV).

pollutant and its reaction kinetics. While the concentration considered in this study may be several magnitudes higher than what is naturally found in the environment, the results obtained have shown that as the concentration of the pollutant increases, the degradation efficiency will reduce. For CFX, at initial concentrations of 5 mg/L, 10 mg/L and 20 mg/L the removal efficiencies were > 99 %, 63 %, and 50 % after 8 min as illustrated in Fig. 4 (a). Also, the kinetic constant reduced from 0.58 min^{-1} to 0.09 min^{-1} as the concentrations increased from 5 mg/L to 20 mg/L as shown in Fig. 4 (b).

Meanwhile, the relationship between the initial concentration of CFX and energy yield showed an opposite trend as seen in Fig S3 (b). At the same treatment time, the energy yield increased with the initial concentration of the pollutant. After 8 min plasma treatment, the energy yield observed for 20 mg/L CFX was about 1.04 g/kWh, while 10 mg/L and 5 mg/L gave energy yields of 0.56 g/kWh and 0.42 g/kWh, respectively. Therefore, in this study, as the initial concentration of CFX increased from 5 mg/L to 20 g/mL, the degradation efficiency reduced by half its value while the energy yield increased by more than two times. This is because as the voltage remained at 6 kV, the quantity of oxidative species, including active particles, was constant per unit time at the same discharge conditions. Therefore, as the rate of collisions among CFX molecules increases at higher initial concentrations, the consumption rate of reactive species rises significantly, thereby imposing a limit on degradation efficiency over a prolonged time. However, at low initial concentrations, the degradation efficiency is enhanced since fewer molecules are reacting with the species. This explanation elucidates why the degradation efficiency of CFX exhibited an inverse relationship with an increase in the initial concentration. A similar observation was reported by Wang et al. [41] for the degradation of metronidazole antibiotics by a DBD plasma configuration. Based on the analysis provided above, the initial concentration of 5 mg/L was selected for subsequent experiments.

3.4. Impact of initial pH

The solution pH can influence the rate of degradation of an organic molecule in an aqueous medium [39]. To investigate the impact of solution pH, synthetic CFX solutions were subjected to treatment in the DBD plasma reactor, varying the initial pH values from 2.6 to 9. The relationship between the initial pH and rate constant is presented in Fig. 5. The results show that the rate of degradation of CFX is pH-sensitive, progressing faster at higher alkaline conditions. In a strongly acidic medium (pH 2.6), the rate constant observed was about 0.1 min^{-1}, compared to 0.58 min^{-1} observed in the weak acidic medium (pH 5). Meanwhile, as the initial pH increased from 5 to 9, the rate constant increased only slightly from 0.58 min^{-1} to 0.62 min^{-1}, respectively, within the treatment time considered. These findings indicate that the degradation of CFX was significantly impeded in a highly acidic condition but favoured in both neutral and alkaline conditions. The explanation for this is two-fold. Firstly, considering that the dissociation constant for CFX is 3.53 [48], when the initial pH was below 3.53, CFX existed in the aqueous solution as molecules. Whereas it existed in the form of anions when the pH was higher than 3.53. Studies have shown that anions can readily react with the reactive species generated in a DBD system which will result in a rapid degradation of the organic compound [49]. Secondly, it has been reported that an increased •OH production is favoured under basic pH due to the presence of OH^- ions which could have increased the reaction rate [50].

Fig. 5 (b) shows the change in pH values resulting from the initial pH variations. For the initial pH values of 5, 7, and 9, the final pH converged to approximately 4.7 ± 0.02 in all three conditions. However, at an initial pH of 2.6, the pH variation remained relatively constant for the entire treatment period. Generally, the pH of a solution during atmospheric air plasma treatment decreases due to the formation of nitrogen compounds [51].

3.5. Effect of adding a metal ion catalyst

The efficiency of plasma treatment in generating non-selective •OH radicals makes it an effective method for treating water and wastewater contaminated with persistent organic pollutants. Fenton reaction is a form of advanced oxidation process that leverages on the highly reactive oxidizing ability of •OH generated from the catalytic decomposition of stable oxidants like H_2O_2. This process can be used independently or in combination with plasma treatment to enhance the generation of •OH thus improving the degradation efficiency of organic pollutants [31,32,52,53].

This study investigated the influence of Fe^{2+} as a low-cost metal ion

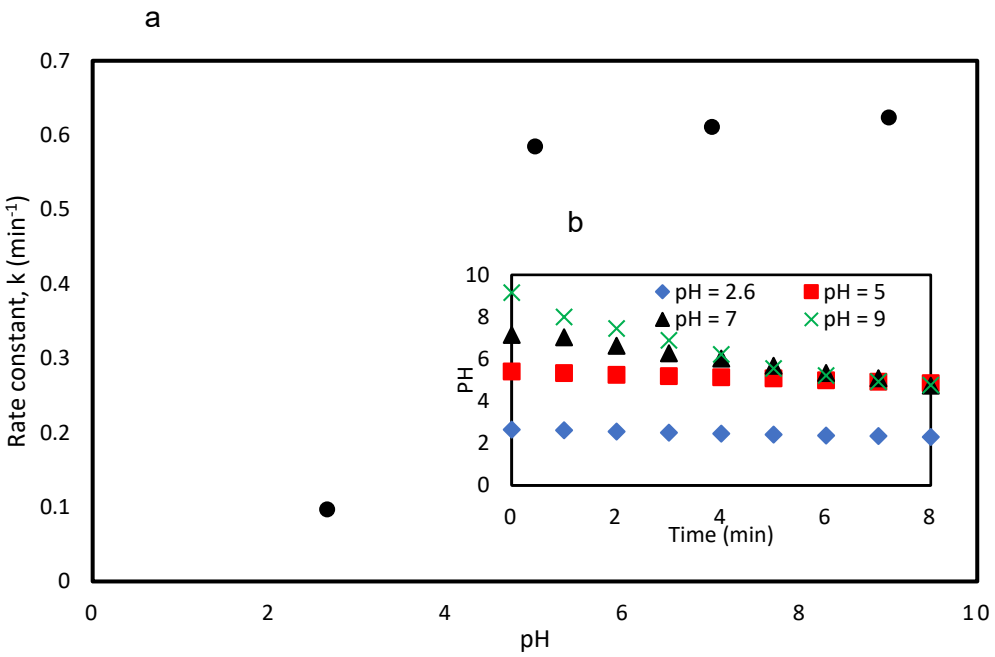

Fig. 5. Effect of initial solution pH on CFX degradation (a) rate constant (b) change in solution pH.

catalyst for the removal of CFX at different concentrations. Fe^{2+} salts, such as ferrous sulfate, are desirable due to their high solubility and reactivity with H_2O_2. As depicted in Fig. 6, the addition of $FeSO_4{\cdot}7H_2O$ (used as the source of Fe^{2+}) resulted in over 99 % degradation of the pollutant in just 4 min. Meanwhile, in the absence of the catalyst, the degradation efficiency was 88 % at the same time period. The accelerated degradation can be attributed to the Fenton reaction occurring in the system [54]. During the discharge process, short-lived •OH recombines to form H_2O_2 in the solution. Subsequently, H_2O_2 reacts with Fe^{2+} according to Eq. (5) to produce more •OH, thereby enhancing the removal of the pollutant. Moreover, as the concentration of Fe^{2+} increased from 10 μmol/L to 100 μmol/L, the rate constant also rose slightly from 1.28 min^{-1} to 1.83 min^{-1} within the treatment period. This increase is due to the augmented production of •OH within the solution, facilitating rapid CFX degradation.

$$Fe^{2+} + H_2O_2 \rightarrow Fe^{3+} + \bullet OH + OH^- \quad (5)$$

It must be mentioned that the "spontaneous" chemical oxidation of ferrous to ferric is strongly dependent on a number of factors including the pH of the aqueous solution. Indeed, it is a complex process involving a variety of partially oxidized *meta*-stable ferrous–ferric intermediate species according to Morgan and Lahav [55]. In our study, the use of atmospheric air (O_2 limiting) as well as the pH of 5 could have limited the oxidation of Fe^{2+} to Fe^{3+} observed by less iron precipitates in the solution.

3.6. Contribution of plasma reactive species and their roles

The efficacy of AOPs like plasma hinges on the generation of reactive chemical species. For an atmospheric air plasma, the spectra profile is primarily characterized by the presence of primary reactive species, including N_2, N_2^+, •OH, and low intensity of O radicals [56]. In an aqueous medium, these reactive chemical species can further facilitate the production of secondary reactive species like H_2O_2, O_3, NO_2^- and NO_3^-. Both O_3 and H_2O_2 were formed from the bombardment of high-energy electrons as seen in Eq. (6) – (10). These represent the long-lived reactive oxygen species (ROS) in the aqueous medium and their concentrations were monitored to explore their roles in the degradation of CFX. These species are also able to generate other highly reactive species, especially •OH, which facilitates the degradation of the pollutant considering its high oxidation potential (E^o = 2.8 V) [57]. According to Fig. 7 (a), the concentration of H_2O_2 is proportional to the treatment time, with an increased rate of H_2O_2 production observed between 6 to 8 min. The maximum H_2O_2 measured was about 1.45 mg/L at 8 min. Meanwhile, the formation of O_3 in the DBD plasma only began after 2 min and maintained a steady growth over the next 6 min reaching a maximum of 0.06 mg/L after 8 min.

$$e^- + O_2 \rightarrow 2 \bullet O + e^- \quad (6)$$

$$e^- + H_2O \rightarrow H \bullet + \bullet OH + e^- \quad (7)$$

$$O_2 + \bullet O \rightarrow O_3 \quad (8)$$

$$\bullet O + H_2O \rightarrow \bullet OH + \bullet OH \quad (9)$$

$$\bullet OH + \bullet OH \rightarrow H_2O_2 \quad (10)$$

The reactive nitrogen species present in the solution are NO_3^- and NO_2^-. These are generated from a series of reactions between excited N_2 with oxygen as presented in Eq. (11) – (16) [58]. The variation of NO_3^- and NO_2^- is shown in Fig. 7 (b). The production of NO_2^- was only observed in the aqueous solution after 4 min of treatment reaching 2 mg/L after 8 min. Whereas, the formation of NO_3^- rose sharply in the first 2 min to 9.5 mg/L, continuing slowly over a prolonged time until 13.6 mg/L in 8 min. The production of the reactive nitrogen species can be linked to the increased acidity of the solution seen in Fig. 5 (b), due to the formation of nitrous and nitric acid [58].

$$N_2 + e^- \rightarrow 2N \bullet + e^- \quad (11)$$

$$O_2 + e^- \rightarrow 2O \bullet + e^- \quad (12)$$

$$N \bullet + O \bullet \rightarrow NO_2 \quad (13)$$

$$2NO + O_2 \rightarrow 2NO_2 \quad (14)$$

$$NO + O_3 \rightarrow NO_2 + O_2 \quad (15)$$

$$NO_2 + NO_2 + H_2O \rightarrow NO_2^- + NO_3^- + 2H^+ \quad (16)$$

To investigate the individual contributions of the key reactive species to the degradation process, individual solutions of CFX containing species-specific scavengers were prepared and subjected to plasma exposure. Based on literature, we selected BQ, TBA, SP, and UA as scavenging agents for $\bullet O_2^-$, •OH, H_2O_2, and O_3, respectively [38,41,56]. The effect of the additions of these scavengers is shown in Fig. 8 (a). In

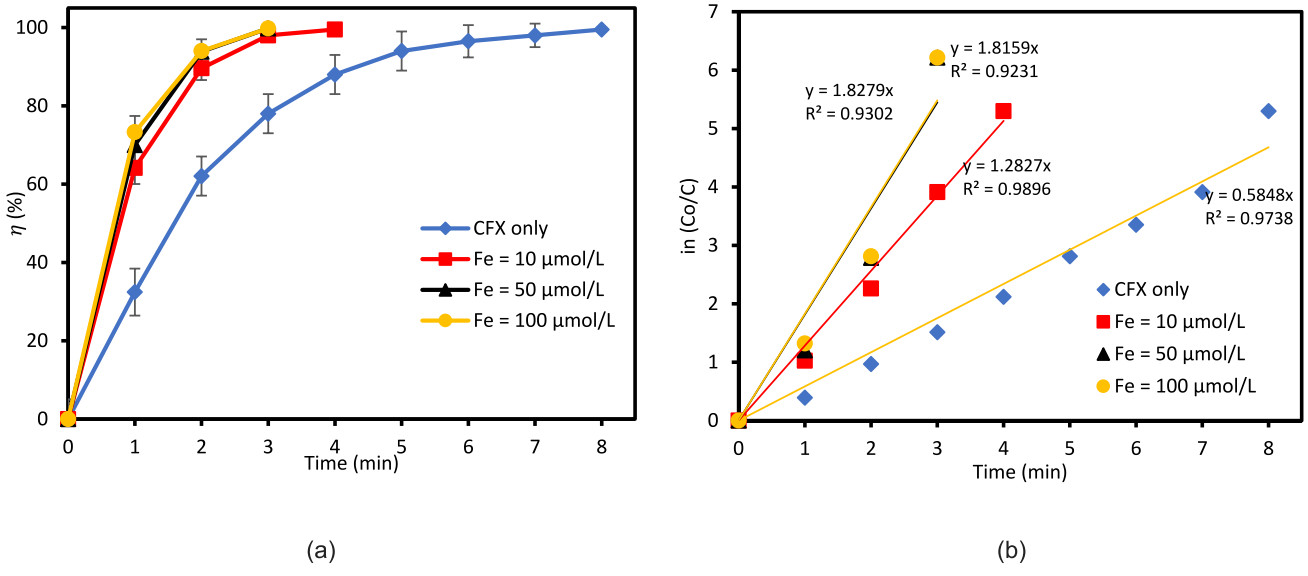

Fig. 6. Effect of Fe^{2+} on the degradation of CFX (a) degradation efficiency (b) kinetics.

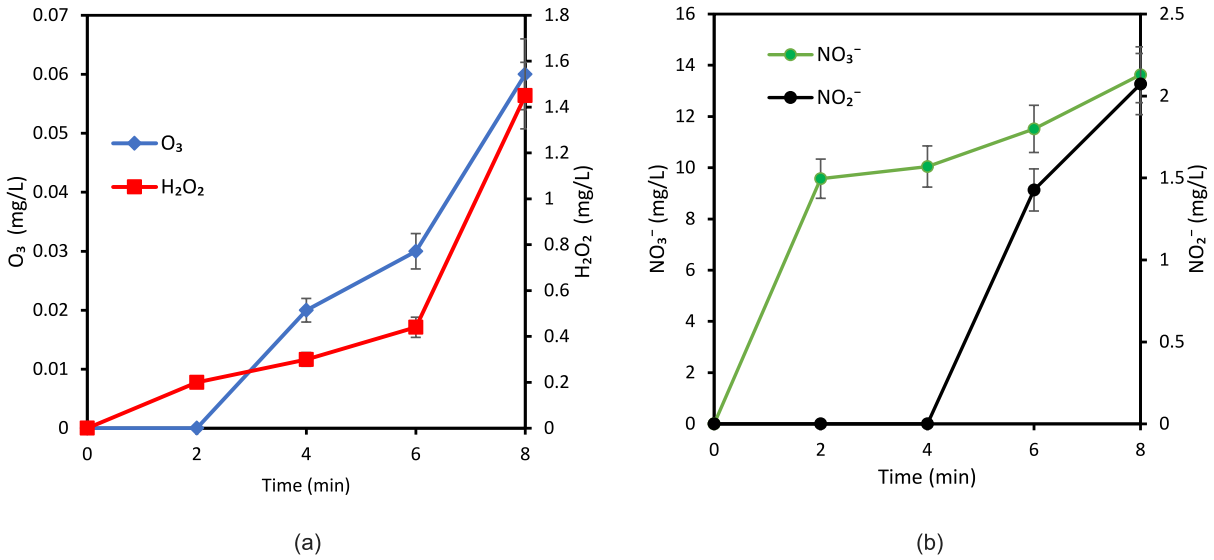

Fig. 7. Contribution of reactive oxygen and nitrogen species during the degradation of CFX (a) O_3 and H_2O_2 (b) NO_3^- and NO_2^-.

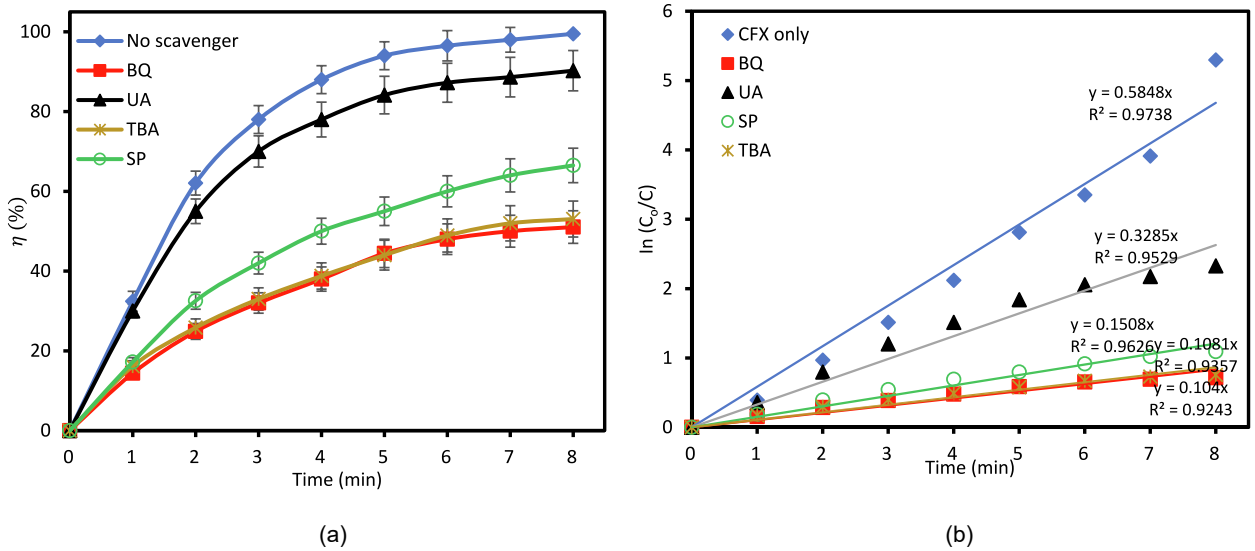

Fig. 8. Effect of scavengers on CFX degradation in the DBD plasma system (a) degradation efficiency (b) rate constants (Initial CFX concentration = 5 mg/L, Voltage = 6 kV, Frequency 20 kHz, Flow rate = 500 mL/min, initial solution pH = 6.0).

this study, 5 mg/L CFX concentration was considered with 0.5 mmol/L concentrations of BQ, TBA, SP, and UA, separately. While this study has only focused on a single dose of the scavengers, further investigation of different concentrations of the quenchants might be necessary to provide an insight into the effect of variations of these scavengers as this could potentially affect the solution properties. The degradation efficiency of CFX was reduced in the presence of the scavengers examined. After 8 min of DBD plasma treatment, the degradation efficiency of CFX reduced from over 99 % (without scavenger) to 90 %, 66 %, 53 %, and 51 % in the presence of UA, TBA, BQ, and SP, respectively. Likewise, the pseudo-first-order kinetic constant was reduced from 0.58 min^{-1} (without scavenger) to 0.33, 0.15, 0.11, and 0.10 min^{-1} upon the addition of UA, SP, TBA, and BQ, respectively. Comparing these results to the control (0.58 min^{-1}), it can be inferred that a significant difference in the degradation efficiency was observed for both TBA and BQ, which suggests that $\bullet O_2^-$ and •OH are the most critical reactive species for CFX degradation in this study. In contrast, O_3 played a minor role in the degradation of CFX, as seen in Fig. 8 (a). Meanwhile, H_2O_2 may also have played a role in the degradation of the pollutant considering that •OH exists for a short time and they combine quickly to generate the species according to Eq. (10).

3.7. *Investigating the combined effect of •OH scavengers and metal ion catalyst*

It has been established in this study that the degradation of the CFX pollutant with an atmospheric air DBD plasma can be related to the amount of H_2O_2 and •OH present. Also, the addition of Fe^{2+} as little as 10 μmol/L concentration was able to influence the rate of degradation of the pollutant through its reaction with H_2O_2 to generate more •OH species. Tert-butyl alcohol and *iso*-propyl alcohol are known •OH scavengers in aqueous solution which can react with the species according to Eq. (17) – (18), respectively. However, the scavenging effect of these species differs. According to Fig. 9 (a) and (b), the addition of 0.5 mmol/L of both TBA and IPA reduced the degradation efficiency of CFX in the aqueous solution to 53 % and 89 % within the treatment time, respectively. The result obtained for IPA in this case is interesting, as a previous study had reported a significant reduction in the degradation of

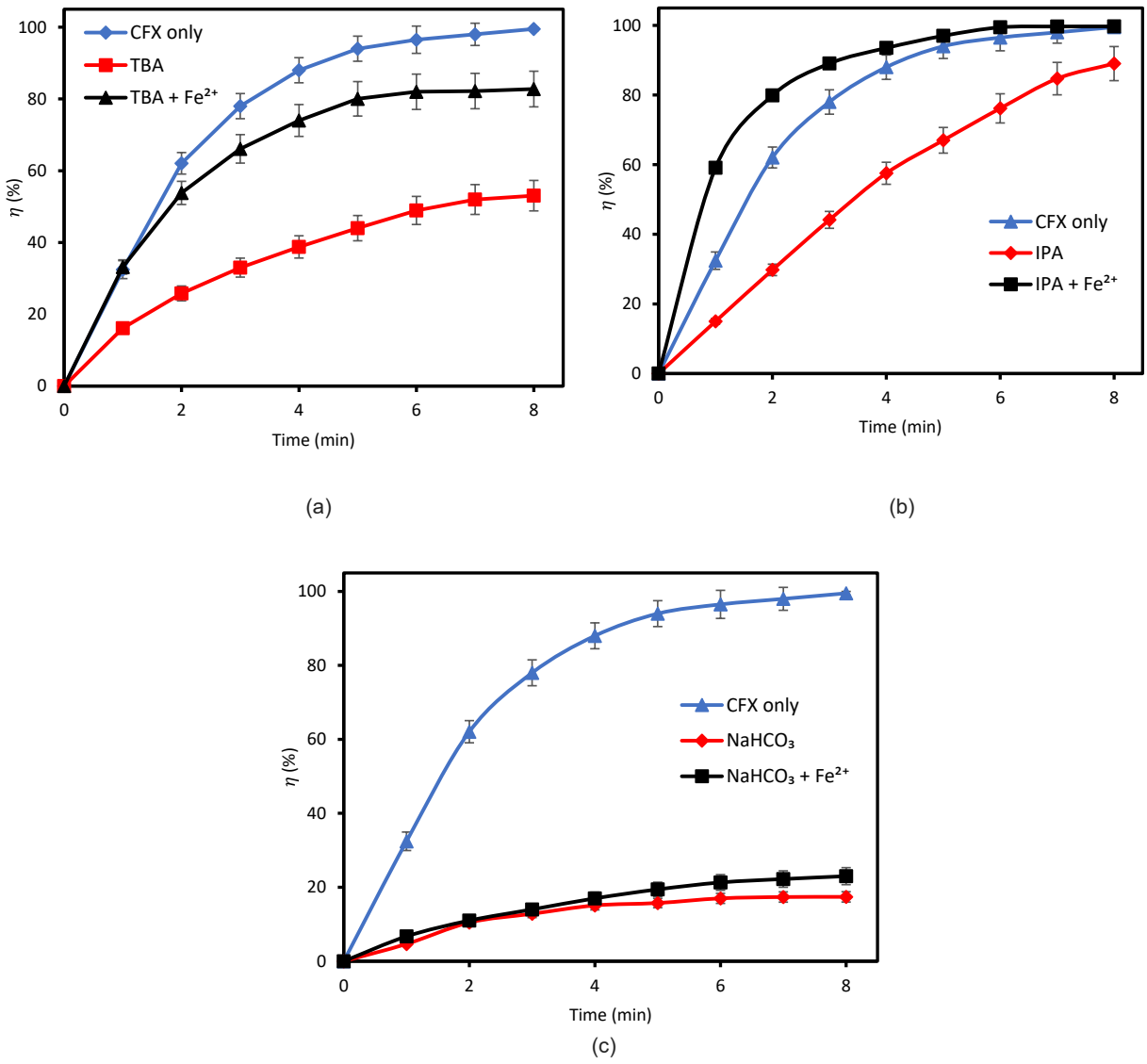

Fig. 9. Effect of different additives on the degradation efficiency of CFX (a) TBA and Fe^{2+} (b) IPA and Fe^{2+} (c) $NaHCO_3$ and Fe^{2+} (Initial CFX concentration = 5 mg/L, Voltage = 6 kV, Frequency 20 kHz, Flow rate = 500 mL/min, initial solution pH = 6.0).

CFX with the addition of the scavenger using a micro-bubble plasma technology [35]. Rong and Sun [59], on the other hand, observed that the addition of IPA improved the removal of triallyl isocyanurate (TAIC) better than the case without the scavenger. In this case, the improved degradation efficiency of TAIC was due to the presence of other reactive species like •H and H_2O_2 even in the absence of •OH. This result supports what was observed in this study because the presence of H_2O_2 was found to be perhaps another contributor to the degradation of CFX.

Also, the difference in the degradation efficiency of IPA and TBA in the aqueous solution can be explained by their reaction constants with •OH. From Eq. (17) and (18), the rate at which IPA ($k = 1.9 \times 10^{10}$ $M^{-1}s^{-1}$) reacts with •OH is faster than that of TBA ($k = 6.0 \times 10^{8}$ $M^{-1}s^{-1}$), respectively [60]. This suggests that IPA has more potential to capture more •OH in the solution, leaving more H_2O_2 to appear in the solution. Also, $NaHCO_3$, which is another other potential scavenger for •OH was considered in this study since it reacts with the reactive species to form carbonate radical ($CO_3^{\bullet}$) according to Eq. (19) [61]. However, despite that $CO_3^{\bullet}$ has a lower oxidizing potential compared to •OH, it can also be a good oxidizing agent. The addition of $NaHCO_3$ limited the degradation of CFX, yielding only 17 % degradation efficiency after 8 min according to Fig. 9 (c).

$$(CH_3)_2CHOH + \bullet OH \rightarrow (CH_3)_2COH + H_2O \; k = 1.9 \times 10^{10}\ M^{-1}s^{-1} \quad (17)$$

$$(CH_3)_3COH + \bullet OH \rightarrow \bullet CH_2C(CH_3)_2OH + H_2O \; k = 6.0 \times 10^{8}\ M^{-1}s^{-1} \quad (18)$$

$$HCO_3^- + \bullet OH \rightarrow CO_3^{\bullet} + H_2O \; k = 8.5 \times 10^{6}\ M^{-1}s^{-1} \quad (19)$$

Fig. 10 (a) – (c) shows the concentrations of H_2O_2 measured in the presence of various chemical additives. Generally, it was observed that more H_2O_2 was detected in the presence of TBA, IPA, and $NaHCO_3$. This signifies that all of these •OH scavengers can enhance the formation of H_2O_2 in the aqueous solution. To explain this observation, first, we considered that the reaction rate constants for Eq. (21) and (22) are 4.5 $\times 10^{9}$ $M^{-1}s^{-1}$ and 2 – 3.8 $\times 10^{7}$ $M^{-1}s^{-1}$, respectively [62], indicating that the rate of recombination of •OH is about 100 times more than the consumption of H_2O_2. This suggests why H_2O_2 may be predominant in the aqueous solution,. Secondly, when •OH is scavenged, the possibility of consuming H_2O_2 based on Eq. (22) becomes minimal, leading to more H_2O_2 available in the aqueous solution. Therefore, considering the mechanism for Fenton reaction described in Eq. (4), H_2O_2 becomes used up as Fe^{2+} catalyst was mixed with TBA, IPA, and $NaHCO_3$ as shown in Fig. 10 (a) – (c).

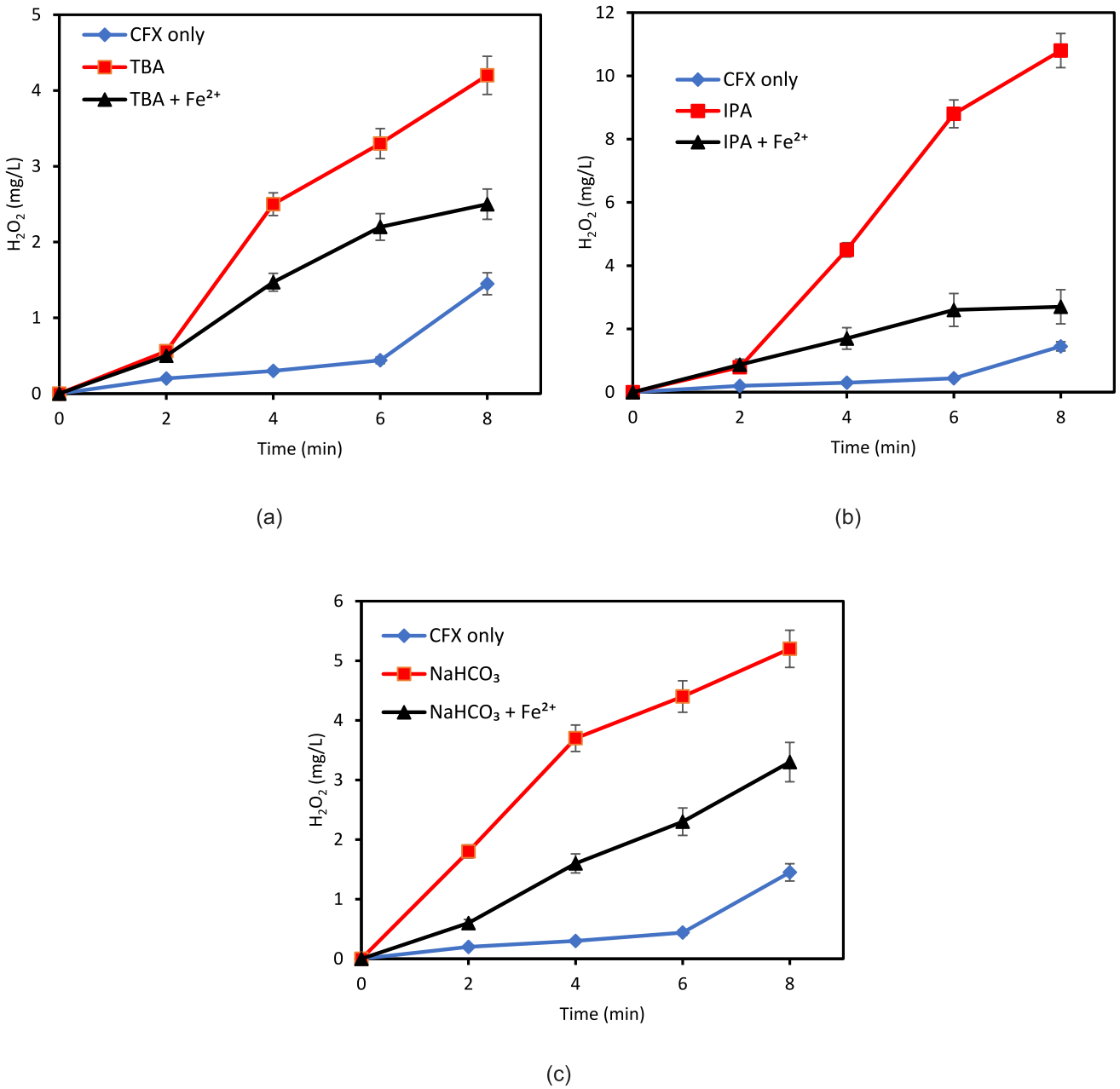

Fig. 10. Effect of various additives on H_2O_2 concentration (a) TBA and Fe^{2+} (b) IPA and Fe^{2+} (c) $NaHCO_3$ and Fe^{2+} (Initial CFX concentration = 5 mg/L, Voltage = 6 kV, Frequency 20 kHz, Flow rate = 500 mL/min, initial solution pH = 6.0).

$$\bullet OH + \bullet H \rightarrow H_2Ok = 7 \times 10^9\ M^{-1}s^{-1} \quad (20)$$

$$\bullet OH + \bullet OH \rightarrow H_2O_2k = 4.5 \times 10^9\ M^{-1}s^{-1} \quad (21)$$

$$H_2O_2 + \bullet OH \rightarrow H_2O \bullet k = 2 - 3.8 \times 10^7\ M^{-1}s^{-1} \quad (22)$$

In addition, when the Fe^{2+} catalyst was mixed with the three scavengers individually, it was observed that the degradation efficiency and kinetics increased, respectively, according to Fig. 9 and Fig. 11. Again, IPA showed the most significant increase and even overlapped the solution without additives. This was because there was more H_2O_2 in the solution which could react with Fe^{2+} to generate more OH radicals. The degradation efficiency with the TBA solution increased from 53 % to 83 %, while $NaHCO_3$ only increased from 17 % to 23 % in the presence of Fe^{2+}. Also, the rate of the reactions and energy yields in the presence of TBA, IPA, and $NaHCO_3$ were reduced according to Fig. 11. However, when Fe^{2+} was introduced, the kinetics observed in the TBA solution had the highest growth of approximately 381 %, while IPA and $NaHCO_3$ increased by 216 % and 33 %, respectively. For the energy yield (g/kWh), IPA and $NaHCO_3$ with Fe^{2+} increased by 21 % and 12.5 %, whereas TBA showed a 54 % increase over the treatment period.

3.8. Identification of degradation intermediates and possible degradation pathways

To clarify the degradation pathway of CFX using plasma, LC-MS analysis was employed to identify intermediate products in the process and the corresponding mass spectrum shown in Fig. S7. A m/z value of 454 was observed at a retention time of 3.55 min which corresponds to the CFX parent compound and other five intermediate compounds with m/z values of 144, 118, 128, 287, and 288 were recognized at various retention times as shown in Table S2 and predicted toxicity

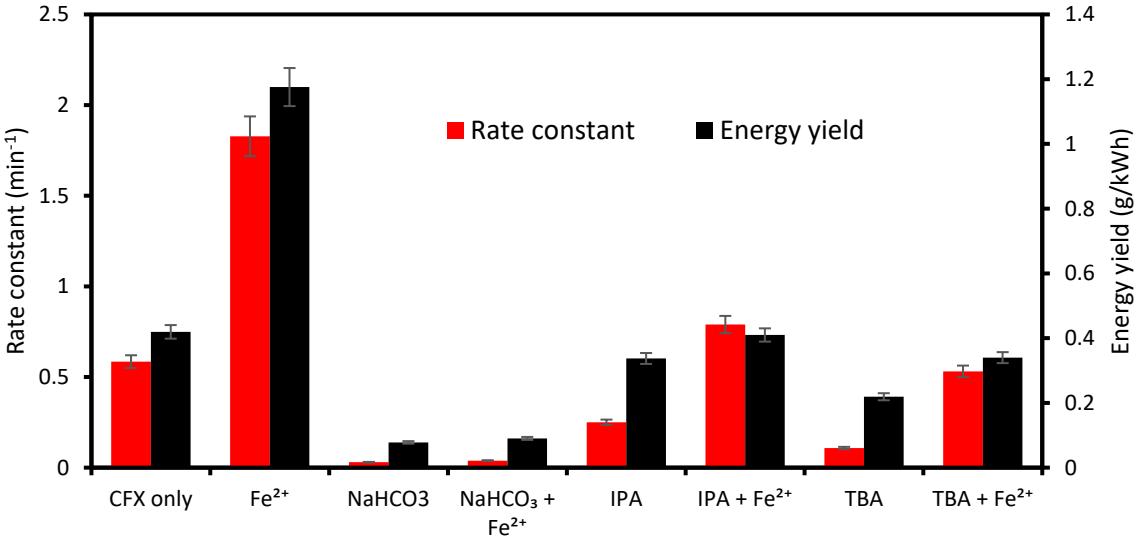

Fig. 11. The rate constant and energy yield under different additives.

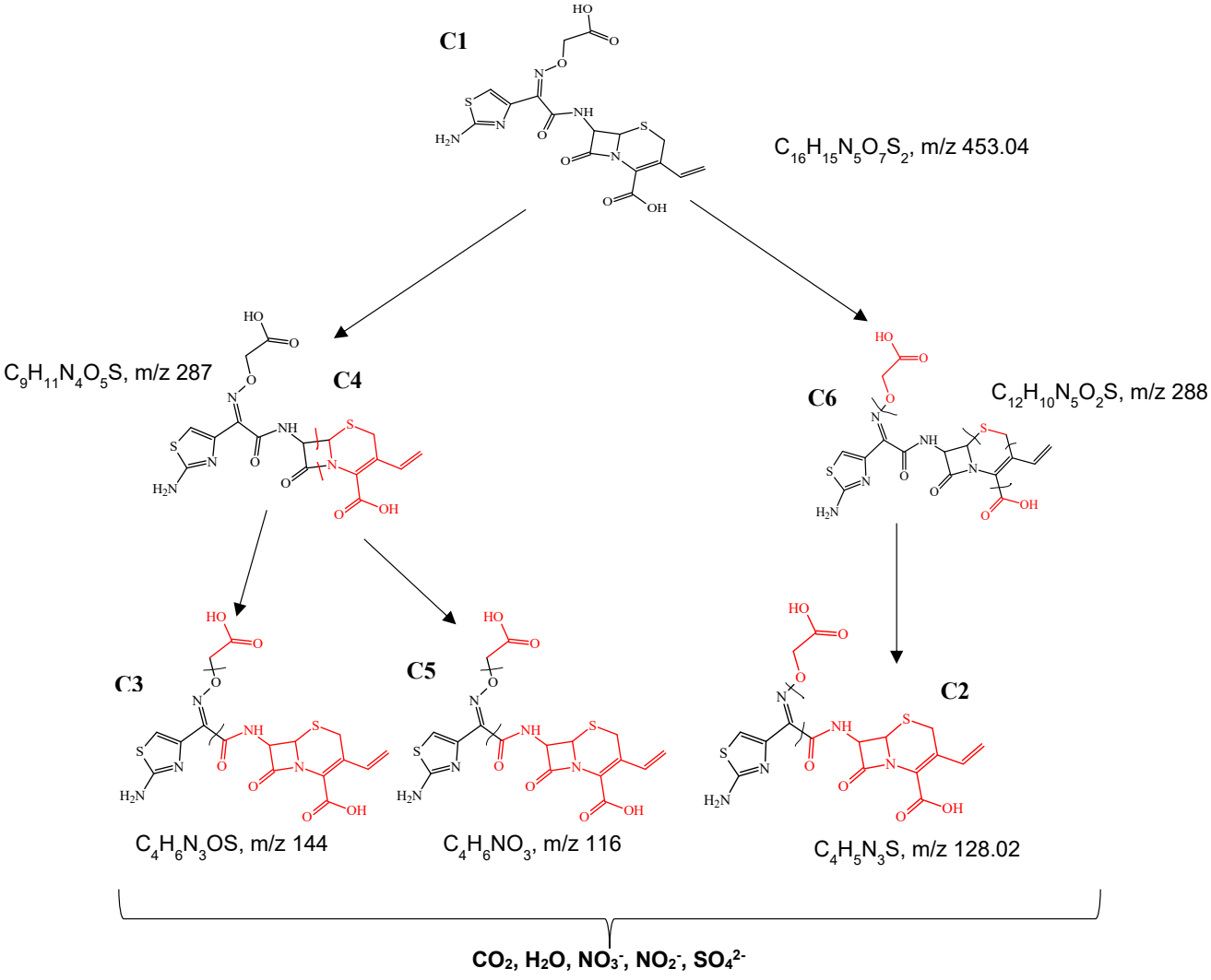

Fig. 12. Proposed degradation pathway for the degradation of CFX using the DBD plasma reactor.

using the Toxicity Estimation Software Tool (T.E.S.T Version 5.1.1) is presented in Table S3 and Fig. S8. The respective peaks have been low considering the concentrations analysed. However, the intensity of the CFX peak decreased with an increase in the treatment times whereas the intensity of the intermediates increased at early stages and decreased thereafter, suggesting their mineralization at later stages of the reaction. The *m/z* values and possible molecular structures of intermediates (Fig. 12) indicate that intermediates were generated mainly through loss of functional groups and ring-open reactions with the main reaction sites as the sulfide in the thiazine ring, carboxylic, amide, and imine groups. The cleavage of the azetidine ring is also suggested. Two degradation pathways have been suggested; one involves cleavage of the azetidine ring to form the first intermediate with an *m/z* value of 287 followed by decarboxylation and cleavage of the imine-amide bond and breaking off of the thiazole ring to form *m/z* 144 and *m/z* 118 respectively. The second pathway involves the opening of the thiazine ring and decarboxylation to form an *m/z* value of 288 followed by cleavage at the amide functional group to form *m/z* 128. Out of the five intermediates, 4 had a shorter retention time than CFX implying that more polar intermediates were produced during degradation due to loss of some functional groups. After 8 min reaction time, some of the intermediates were eventually converted to H_2O, CO_2, NO_3^-, NO_2^-, and SO_4^{2-}. At this reaction time, the spectra suggest that there might be an incomplete mineralization since small amounts of intermediates (*m/z* 144 and *m/z* 128) are still present but can fully be mineralized with a longer degradation time.

4. Conclusion

An atmospheric air dielectric barrier discharge reactor was used in the degradation of cefixime antibiotics in this study. The results demonstrated that the pollutant can be almost completely removed by the technology in 8 min treatment time using an AC power supply operated at 6 kV applied voltage and 20 kHz frequency. An energy yield of 0.42 g/kWh was obtained with the reactor. The active species responsible for the degradation of this pollutant are primarily •OH and $\bullet O_2^-$ which were identified via radical scavenger experiments·H_2O_2 also played a minor role in the degradation of the pollutant. The influence of Fe^{2+} catalyst improved the oxidizing power of H_2O_2 generated by the reactor through its conversion to •OH which enhanced the degradation of CFX. A new contribution was also made with regards to the application of a DBD plasma reactor which is an investigation of the mixed additives of hydroxyl radical scavengers and the metal ion catalyst. From the degradation of cefixime, 5 intermediate products were observed which were used in proposing a degradation pathway.

CRediT authorship contribution statement

Samuel O. Babalola: Writing – review & editing, Writing – original draft, Methodology, Investigation, Formal analysis, Conceptualization. **Paul A. Steenkamp:** Methodology. **Michael O. Daramola:** Writing – review & editing, Supervision. **Samuel A. Iwarere:** Writing – review & editing, Validation, Methodology, Funding acquisition, Data curation.

Declaration of competing interest

The authors declare that they have no known competing financial interests or personal relationships that could have appeared to influence the work reported in this paper.

Data availability

Data will be made available on request.

Acknowledgement

This research was supported by the Government of the United Kingdom through The Royal Society FLAIR award [FLR\R1\201683]. The byproduct analysis was conducted at the Council for Scientific and Industrial Research (CSIR), South Africa under the supervision of Professor Paul A. Steenkamp. Hilda Kyomuhimbo also assisted with the identification of the degradation byproducts and proposition of a degradation pathway.

Appendix A. Supplementary material

Supplementary data to this article can be found online at https://doi.org/10.1016/j.seppur.2024.128376.

References

[1] L. Wang, C. Wang, Q. Liu, Q. Meng, X. Huo, P. Sun, et al., PEPT1- and OAT1/3-mediated drug-drug interactions between bestatin and cefixime in vivo and in vitro in rats, and in vitro in human, Eur. J. Pharm. Sci. 63 (2014) 77–86, https://doi.org/10.1016/j.ejps.2014.06.019.
[2] V. Hasanzadeh, O. Rahmanian, M. Heidari, Cefixime adsorption onto activated carbon prepared by dry thermochemical activation of date fruit residues, Microchem. J. 152 (2020) 104261, https://doi.org/10.1016/j.microc.2019.104261.
[3] R. Kafaei, F. Papari, M. Seyedabadi, S. Sahebi, R. Tahmasebi, Occurrence, distribution, and potential sources of antibiotics pollution in the water-sediment of the northern coastline of the Persian Gulf, Iran, Sci. Total Environ 627 (2018) 703–712, https://doi.org/10.1016/j.scitotenv.2018.01.305.
[4] Y. Yang, Y.I. Cho, A. Fridman, Plasma Discharge in Liquid: Water Treatment and Applications, Taylor & Francis Group, 2012.
[5] Adamovich I, Baalrud SD, Bogaerts A, Bruggeman PJ, Cappelli M, Colombo V, et al. The 2017 Plasma Roadmap: Low temperature plasma science and technology. J Phys D Appl Phys 2017;50. Doi: 10.1088/1361-6463/aa76f5.
[6] M. Saleem, O. Biondo, G. Sretenović, G. Tomei, M. Magarotto, D. Pavarin, et al., Comparative performance assessment of plasma reactors for the treatment of PFOA; reactor design, kinetics, mineralization and energy yield, Chem. Eng. J. 382 (2020) 123031, https://doi.org/10.1016/j.cej.2019.123031.
[7] D. Nikitin, B. Kaur, S. Preis, N. Dulova, Persulfate contribution to photolytic and pulsed corona discharge oxidation of metformin and tramadol in water, Process Saf. Environ. Prot. 165 (2022) 22–30, https://doi.org/10.1016/j.psep.2022.07.002.
[8] D. Dobrin, M. Magureanu, C. Bradu, N.B. Mandache, P. Ionita, V.I. Parvulescu, Degradation of methylparaben in water by corona plasma coupled with ozonation, Environ. Sci. Pollut. Res. (2014) 12190–12197, https://doi.org/10.1007/s11356-014-2964-y.
[9] K.H.H. Aziz, H. Miessner, A. Mahyar, S. Mueller, D. Moeller, F. Mustafa, et al., Degradation of perfluorosurfactant in aqueous solution using non-thermal plasma generated by nano-second pulse corona discharge reactor, Arab. J. Chem. 14 (2021) 103366, https://doi.org/10.1016/j.arabjc.2021.103366.
[10] C.A. Aggelopoulos, S. Meropoulis, M. Hatzisymeon, Z.G. Lada, G. Rassias, Degradation of antibiotic enrofloxacin in water by gas-liquid nsp-DBD plasma: Parametric analysis, effect of H2O2 and CaO2 additives and exploration of degradation mechanisms, Chem. Eng. J. 398 (2020) 125622, https://doi.org/10.1016/j.cej.2020.125622.
[11] A.S. Bansode, S.E. More, E.A. Siddiqui, S. Satpute, A. Ahmad, S.V. Bhoraskar, et al., Effective degradation of organic water pollutants by atmospheric non-thermal plasma torch and analysis of degradation process, Chemosphere 167 (2017) 396–405, https://doi.org/10.1016/j.chemosphere.2016.09.089.
[12] S. Li, X. Ma, Y. Jiang, X. Cao, Acetamiprid removal in wastewater by the low-temperature plasma using dielectric barrier discharge, Ecotoxicol. Environ. Saf. 106 (2014) 146–153, https://doi.org/10.1016/j.ecoenv.2014.04.034.
[13] D.R. Merouani, F. Abdelmalek, F. Taleb, M. Martel, A. Semmoud, A. Addou, Plasma treatment by gliding arc discharge of dyes / dye mixtures in the presence of inorganic salts, Arab. J. Chem. 8 (2015) 155–163, https://doi.org/10.1016/j.arabjc.2011.01.034.
[14] M. El-Shaer, M. Mobasher, A. Elsebaei, N. Essam, Gliding arc plasma for environmental friendly treatment of waste water, ResearchGate (2018), https://doi.org/10.13140/RG.2.2.11373.84964.
[15] R. Pelalak, R. Alizadeh, E. Ghareshabani, Enhanced heterogeneous catalytic ozonation of pharmaceutical pollutants using a novel nanostructure of iron-based mineral prepared via plasma technology: A comparative study, J. Hazard. Mater. 392 (2020) 122269, https://doi.org/10.1016/j.jhazmat.2020.122269.
[16] M. Magureanu, D. Piroi, N.B. Mandache, V. David, A. Medvedovici, V.I. Parvulescu, Degradation of pharmaceutical compound pentoxifylline in water by non-thermal plasma treatment, Water Res. 44 (2010) 3445–3453, https://doi.org/10.1016/j.watres.2010.03.020.
[17] J. Zeng, B. Yang, X. Wang, Z. Li, X. Zhang, L. Lei, Degradation of pharmaceutical contaminant ibuprofen in aqueous solution by cylindrical wetted-wall corona discharge, Chem. Eng. J. 267 (2015) 282–288, https://doi.org/10.1016/j.cej.2015.01.030.

[18] S. Karoui, W.A. Saoud, A. Ghorbal, F. Fourcade, A. Amrane, A.A. Assadi, Intensification of non-thermal plasma for aqueous Ciprofloxacin degradation: Optimization study, mechanisms, and combined plasma with photocatalysis, J. Water Process Eng. 50 (2022) 103207, https://doi.org/10.1016/j.jwpe.2022.103207.
[19] Q. Zhang, H. Zhang, Q. Zhang, Q. Huang, Degradation of norfloxacin in aqueous solution by atmospheric-pressure non-thermal plasma: Mechanism and degradation pathways, Chemosphere 210 (2018) 433–439, https://doi.org/10.1016/j.chemosphere.2018.07.035.
[20] R. Banaschik, P. Lukes, H. Jablonowski, M.U. Hammer, K.D. Weltmann, J.F. Kolb, Potential of pulsed corona discharges generated in water for the degradation of persistent pharmaceutical residues, Water Res. 84 (2015) 127–135, https://doi.org/10.1016/j.watres.2015.07.018.
[21] Y. Liu, S. Mei, D. Iya-Sou, S. Cavadias, S. Ognier, Carbamazepine removal from water by dielectric barrier discharge: Comparison of ex situ and in situ discharge on water, Chem. Eng. Process. 56 (2012) 10–18, https://doi.org/10.1016/j.cep.2012.03.003.
[22] J.O. Back, T. Obholzer, K. Winkler, S. Jabornig, M. Rupprich, Combining ultrafiltration and non-thermal plasma for low energy degradation of pharmaceuticals from conventionally treated wastewater, J. Environ. Chem. Eng. 6 (2018) 7377–7385, https://doi.org/10.1016/j.jece.2018.07.047.
[23] J. Foster, B.S. Sommers, S.N. Gucker, I.M. Blankson, G. Adamovsky, Perspectives on the interaction of plasmas with liquid water for water purification, IEEE Trans. Plasma Sci. 40 (2012) 1311–1323, https://doi.org/10.1109/TPS.2011.2180028.
[24] C.A. Aggelopoulos, C.D. Tsakiroglou, A new perspective towards in-situ cold plasma remediation of polluted sites: Direct generation of micro-discharges within contaminated medium, Chemosphere 266 (2021) 128969, https://doi.org/10.1016/j.chemosphere.2020.128969.
[25] L. Gao, X. Shi, X. Wu, Applications and challenges of low temperature plasma in pharmaceutical field, J. Pharm. Anal. 11 (2021) 28–36, https://doi.org/10.1016/j.jpha.2020.05.001.
[26] C. Subrahmanyam, M. Magureanu, A. Renken, L. Kiwi-Minsker, Catalytic abatement of volatile organic compounds assisted by non-thermal plasma. Part 1. A novel dielectric barrier discharge reactor containing catalytic electrode, Appl. Catal. B Environ. 65 (2006) 150–156, https://doi.org/10.1016/j.apcatb.2006.01.006.
[27] J. Wang, Y. Sun, J. Feng, L. Xin, J. Ma, Degradation of triclocarban in water by dielectric barrier discharge plasma combined with TiO2/activated carbon fibers: Effect of operating parameters and byproducts identification, Chem. Eng. J. 300 (2016) 36–46, https://doi.org/10.1016/j.cej.2016.04.041.
[28] M. Russo, G. Iervolino, V. Vaiano, V. Palma, Non-thermal plasma coupled with catalyst for the degradation of water pollutants: A review, Catalysts 10 (2020) 1–29, https://doi.org/10.3390/catal10121438.
[29] P. Manoj Kumar Reddy, S. Mahammadunnisa, C. Subrahmanyam, Catalytic non-thermal plasma reactor for mineralization of endosulfan in aqueous medium: A green approach for the treatment of pesticide contaminated water, Chem. Eng. J. 238 (2014) 157–163, https://doi.org/10.1016/j.cej.2013.08.087.
[30] L. Chandana, C.J. Sangeetha, T. Shashidhar, C. Subrahmanyam, Non-thermal atmospheric pressure plasma jet for the bacterial inactivation in an aqueous medium, Sci. Total Environ. 640–641 (2018) 493–500, https://doi.org/10.1016/j.scitotenv.2018.05.342.
[31] K. Hsieh, H. Wang, B.R. Locke, Analysis of a gas-liquid film plasma reactor for organic compound oxidation, J. Hazard. Mater. 317 (2016) 188–197, https://doi.org/10.1016/j.jhazmat.2016.05.053.
[32] K.H. Hama Aziz, H. Miessner, S. Mueller, D. Kalass, D. Moeller, I. Khorshid, et al., Degradation of pharmaceutical diclofenac and ibuprofen in aqueous solution, a direct comparison of ozonation, photocatalysis, and non-thermal plasma, Chem. Eng. J. 313 (2017) 1033–1041, https://doi.org/10.1016/j.cej.2016.10.137.
[33] D.B. Luiz, A.K. Genena, E. Virmond, H.J. José, R.F.P.M. Moreira, W. Gebhardt, et al., Identification of degradation products of Erythromycin A arising from ozone and advanced oxidation process treatment, Water Environ. Res. 82 (2010) 797–805, https://doi.org/10.2175/106143010x12609736966928.
[34] G.R. Stratton, F. Dai, C.L. Bellona, T.M. Holsen, E.R.V. Dickenson, T.S. Mededovic, Plasma-based water treatment: Efficient transformation of perfluoroalkyl substances in prepared solutions and contaminated groundwater, Environ. Sci. Tech. 51 (2017) 1643–1648, https://doi.org/10.1021/acs.est.6b04215.
[35] T. Zhang, R. Zhou, P. Wang, A. Mai-prochnow, R. Mcconchie, W. Li, et al., Degradation of cefixime antibiotic in water by atmospheric plasma bubbles : Performance, degradation pathways and toxicity evaluation, Chem. Eng. J. 421 (2021) 127730, https://doi.org/10.1016/j.cej.2020.127730.
[36] S.O. Babalola, M.O. Daramola, S.A. Iwarere, An investigation on the removal of tramadol analgesic in deionized water and final wastewater effluent using a novel continuous flow dielectric barrier discharge reactor, J. Water Process Eng. 56 (2023) 104294, https://doi.org/10.1016/j.jwpe.2023.104294.
[37] P. Murugesan, V. Evanjalin Monica, J.A. Moses, C. Anandharamakrishnan, Water decontamination using non-thermal plasma: Concepts, applications, and prospects, J. Environ. Chem. Eng. (2020) 8, https://doi.org/10.1016/j.jece.2020.104377.
[38] Z. Li, Y. Wang, H. Guo, S. Pan, C. Puyang, Y. Su, et al., Insights into water film DBD plasma driven by pulse power for ibuprofen elimination in water: performance, mechanism and degradation route, Sep. Purif. Technol. 277 (2021) 119415, https://doi.org/10.1016/j.seppur.2021.119415.
[39] Z. Yu, Y. Sun, G. Zhang, C. Zhang, Degradation of DEET in aqueous solution by water falling film dielectric barrier discharge: Effect of three operating modes and analysis of the mechanism and degradation pathway, Chem. Eng. J. 317 (2017) 90–102, https://doi.org/10.1016/j.cej.2017.02.068.
[40] P. Verlicchi, V. Grillini, Surface water and groundwater quality in South Africa and Mozambique — Analysis of the most critical pollutants for drinking purposes and challenges in water treatment selection, Water (2020), https://doi.org/10.3390/w12010305.
[41] B. Wang, X. Li, Y. Wang, Degradation of metronidazole in water using dielectric barrier discharge synergistic with sodium persulfate, Sep. Purif. Technol. 303 (2022) 122173, https://doi.org/10.1016/j.seppur.2022.122173.
[42] B. Erim, Z. Ciğeroğlu, S. Şahin, Y. Vasseghian, Photocatalytic degradation of cefixime in aqueous solutions using functionalized SWCNT/ZnO/Fe3O4 under UV-A irradiation, Chemosphere (2022) 291, https://doi.org/10.1016/j.chemosphere.2021.132929.
[43] M. Swedha, M.K. Okla, M.A. Abdel-Maksoud, S. Kokilavani, K. Kamwilaisak, M. Sillanpää, et al., Photo-Fenton system Fe3O4/NiCu2S4 QDs towards bromoxynil and cefixime degradation: A realistic approach, Surf. Interfaces (2023) 38, https://doi.org/10.1016/j.surfin.2023.102764.
[44] Z. Ur Rahman, U. Shah, A. Alam, Z. Shah, K. Shaheen, S. Bahadar Khan, et al., Photocatalytic degradation of cefixime using CuO-NiO nanocomposite photocatalyst, Inorg. Chem. Commun. 148 (2023) 110312, https://doi.org/10.1016/j.inoche.2022.110312.
[45] N.M. Shooshtari, M.M. Ghazi, An investigation of the photocatalytic activity of nano A-Fe2O3/ZnO on the photodegradation of cefixime trihydrate, Chem. Eng. J. 315 (2017) 527–536, https://doi.org/10.1016/j.cej.2017.01.058.
[46] A. Pourtaheri, A. Nezamzadeh-Ejhieh, Photocatalytic properties of incorporated NiO onto clinoptilolite nano-particles in the photodegradation process of aqueous solution of cefixime pharmaceutical capsule, Chem. Eng. Res. Des. 104 (2015) 835–843, https://doi.org/10.1016/j.cherd.2015.10.031.
[47] Rasouli K, Alamdari A, Sabbaghi S. Ultrasonic-assisted synthesis of α-Fe2O3@TiO2 photocatalyst: Optimization of effective factors in the fabrication of photocatalyst and removal of non-biodegradable cefixime via response surface methodology-central composite design. Sep Purif Technol 2023;307. Doi: 10.1016/j.seppur.2022.122799.
[48] N. Sanli, S. Sanli, U. Sızır, M. Gumustas, S.A. Ozkan, Determination of pK a values of cefdinir and cefixime by LC and spectrophotometric methods and their analysis in pharmaceutical dosage forms, Chromatographia 73 (2011) 1171–1176, https://doi.org/10.1007/s10337-011-2013-7.
[49] J. Hoigné, H. Bader, Rate constants of reactions of ozone with organic and inorganic compounds in water-I. Non-dissociating organic compounds, Water Res. 17 (1983) 173–183, https://doi.org/10.1016/0043-1354(83)90098-2.
[50] B. Sun, M. Sato, J.S. Clements, Optical study of active species produced by a pulsed streamer corona discharge in water, J. Electrostat. 39 (1997) 189–202, https://doi.org/10.1016/S0304-3886(97)00002-8.
[51] S.P. Rong, Y.B. Sun, Z.H. Zhao, Degradation of sulfadiazine antibiotics by water falling film dielectric barrier discharge, Chin. Chem. Lett. 25 (2014) 187–192, https://doi.org/10.1016/j.cclet.2013.11.003.
[52] K.H. Hama Aziz, A. Mahyar, H. Miessner, S. Mueller, D. Kalass, D. Moeller, et al., Application of a planar falling film reactor for decomposition and mineralization of methylene blue in the aqueous media via ozonation, Fenton, photocatalysis and non-thermal plasma: A comparative study, Process Saf. Environ. Prot. 113 (2018) 319–329, https://doi.org/10.1016/j.psep.2017.11.005.
[53] S. Slamani, F. Abdelmalek, M.R. Ghezzar, A. Addou, Initiation of Fenton process by plasma gliding arc discharge for the degradation of paracetamol in water, J. Photochem. Photobiol. A Chem. 359 (2018) 1–10, https://doi.org/10.1016/j.jphotochem.2018.03.032.
[54] G. Boczkaj, A. Fernandes, Wastewater treatment by means of advanced oxidation processes based on cavitation – A review, Chem. Eng. J. 320 (2017) 608–633, https://doi.org/10.1016/j.cej.2017.03.084049.
[55] B. Morgan, O. Lahav, The effect of pH on the kinetics of spontaneous Fe(II) oxidation by O2 in aqueous solution - basic principles and a simple heuristic description, Chemosphere 68 (2007) 2080–2084, https://doi.org/10.1016/j.chemosphere.2007.02.015.
[56] S. Meropoulis, S. Giannoulia, S. Skandalis, G. Rassias, C.A. Aggelopoulos, Key-study on plasma-induced degradation of cephalosporins in water: Process optimization, assessment of degradation mechanisms and residual toxicity, Sep. Purif. Technol. 298 (2022) 121639, https://doi.org/10.1016/j.seppur.2022.121639.
[57] S. Lee, J. Lee, W. Nam, G. Yun, Enhanced production of hydroxyl radicals in plasma-treated water via a negative DC bias coupling, J. Phys. D Appl. Phys. 55 (2022) 455201, https://doi.org/10.1088/1361-6463/ac9000.
[58] Allabakshi SM, Srikar PSNSR, Gangwar RK, Maliyekkal SM. Feasibility of surface dielectric barrier discharge in wastewater treatment: Spectroscopic modeling, diagnostic, and dye mineralization. Sep Purif Technol 2022;296:121344. Doi: 10.1016/j.seppur.2022.121344.
[59] S. Rong, Y. Sun, Degradation of TAIC by water falling film dielectric barrier discharge - Influence of radical scavengers, J. Hazard. Mater. 287 (2015) 317–324, https://doi.org/10.1016/j.jhazmat.2015.02.003.
[60] Buxton G V, Greenstock CL, Helman P, Ross AB. Critical Review of Rate Constants for Reactions of Hydrated Electrons , Hydrogen Atoms and Hydroxyl Radicals (· OH /· O-) in Aqueous Solution. J Phys Chem Ref Data 1988;17. https://doi.org/Doi: 10.1063/1.555805.
[61] E. Marotta, E. Ceriani, M. Schiorlin, C. Ceretta, C. Paradisi, Comparison of the rates of phenol advanced oxidation in deionized and tap water within a dielectric barrier discharge reactor, Water Res. 46 (2012) 6239–6246, https://doi.org/10.1016/j.watres.2012.08.022.
[62] M. Sahni, B.R. Locke, Quantification of hydroxyl radicals produced in aqueous phase pulsed electrical discharge reactors, Ind. Eng. Chem. Res. 45 (2006) 5819–5825, https://doi.org/10.1021/ie0601504.